

Hip and Pelvis



Nele Herregods, Jacob Jaremko, and Lennart Jans

Introduction

The hip of the child is not a miniature adult hip. In immature hips, the structures that later will result in the neck, head, and greater trochanter are initially cartilaginous and progressively ossify (Fig. 1a). The greater trochanter and the femoral head are completely ossified by the age of 12. The femoral head and greater trochanter share the same growth plate that closes only after puberty. The blood perfusion of the femoral head in children depends solely on an arterial anastomotic network in the posterior region of the femoral neck. There is no flow to the

N. Herregods (✉)

Department of Radiology and Nuclear Medicine, Ghent University Hospital, Ghent, Belgium

e-mail: nele.herregods@uzgent.be

J. Jaremko

Department of Radiology, University of Alberta, Edmonton, AB, Canada

L. Jans

Department of Radiology and Nuclear Medicine, Ghent University Hospital, Ghent, Belgium

© The Author(s), under exclusive license to Springer Nature Switzerland AG 2023

P. Simoni, M. P. Aparisi Gómez (eds.), *Essential Measurements in Pediatric Musculoskeletal Imaging*,

https://doi.org/10.1007/978-3-031-17735-4_8

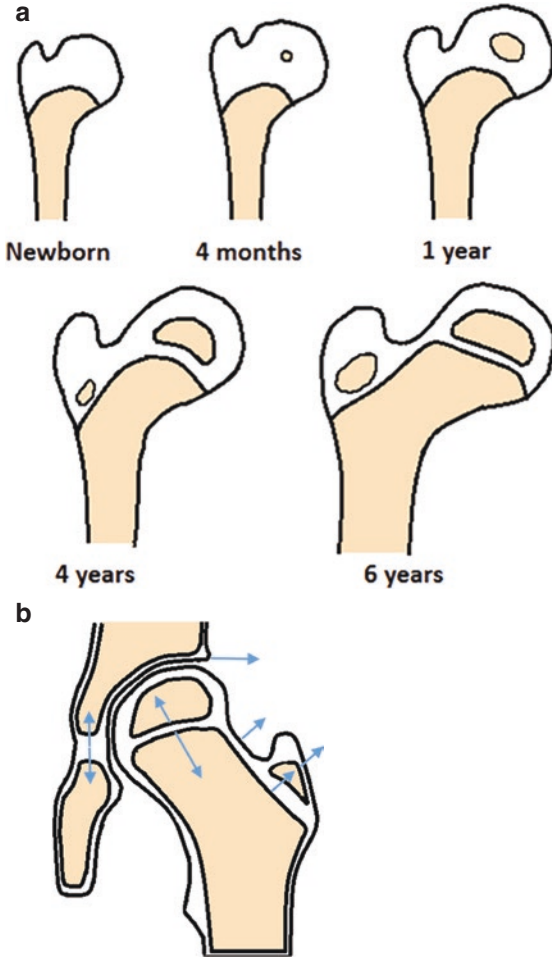


FIGURE 1 (a) Schematic representation of the growing human proximal femur, showing the femoral head and greater trochanter ossification centers at different ages. (b) Growth of the hip: The acetabulum grows in depth and width from the triradiate cartilage and by apposition from the edge. A secondary ossification center at the edge of the acetabulum appears in the early second decade, known as os acetabuli. The greater trochanter enlarges by physal growth up to 8 years of age, after which growth is appositional. Acetabulum and greater trochanter growth is physal and appositional. (With permission from Herregods et al. [1])

femoral head due to the presence of a growth plate. Only in children below 18 months, there are transphyseal vessels to the epiphysis. There is growth in the transition area from the head to the femoral neck (growth cartilage), responsible for normal growth of the femoral head and neck lengthening, growth cartilage in the greater trochanter, and the triradiate growth cartilage of the acetabulum that grows in depth and width so as to maintain its sphericity and concavity and hold the femoral head in joint (Fig. 1b). Lesion or trauma of these regions may predispose to severe anomalies in the development of the femoral head or deformities of the acetabulum [1, 2].

Developmental Dysplasia (DDH)

- In children >5–6 months of age, radiography is indicated because progressing ossification of the femoral head prevents adequate evaluation with US [3].
- For infants <4–5 months of age, ultrasound (US) is still the imaging modality of choice [4, 5].
- Several lines and angles are used to diagnose and further characterize DDH: Hilgenreiner's, Perkin's, and Shenton's line, and the acetabular and center-edge angle [1, 6].
- A second AP radiograph of the pelvis with the thighs in abduction, flexion, and external rotation (i.e., frog-leg lateral projection) is performed to determine whether a displaced or subluxed hip is reducible [7].

Hip Acetabular Angle

- Measured on anteroposterior (AP) radiograph of the hips in a neutral position.
- Formed by a horizontal line connecting both triradiate cartilages (Hilgenreiner's line) and a second line which extends along the acetabular roofs (Fig. 2).
- In adolescents where the triradiate cartilages are fused and therefore inapparent, the inferior margin of the pelvic teardrop is used instead.
- Normal values for different ages are shown in Table 1 [8].

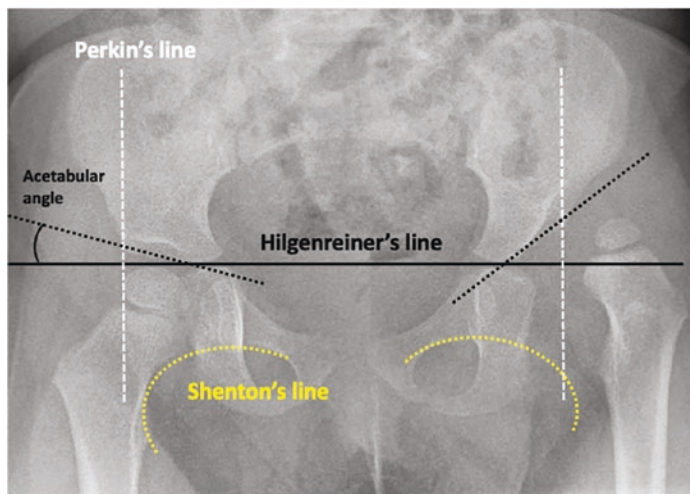


FIGURE 2 Anteroposterior radiograph showing Hilgenreiner's, Perkin's, and Shenton's lines, and the acetabular angle. There is developmental dysplasia of the left hip with increased acetabular angle, a shallow acetabulum, and dislocation. Note delayed ossification of the left femoral head epiphysis. The right hip joint is normal. (Permission from Herregods et al. [1])

TABLE I Normal values of acetabular angles for different ages and sexes [8]

Age	Acetabular angle females	Acetabular angle males
Newborn	$28.8^{\circ} \pm 4.8^{\circ}$	$26.4^{\circ} \pm 4.4^{\circ}$
3 months old	$25^{\circ} \pm 3.5^{\circ}$	$22^{\circ} \pm 4^{\circ}$
6 months old	$23.2^{\circ} \pm 4.0^{\circ}$	$20.3^{\circ} \pm 3.7^{\circ}$
1 year old	$21.2^{\circ} \pm 3.8^{\circ}$	$19.8^{\circ} \pm 3.6^{\circ}$
>2 years old	$18^{\circ} \pm 4^{\circ}$	$19^{\circ} \pm 3.6^{\circ}$

- Perkin's line is a line drawn perpendicular to Hilgenreiner's line, intersecting the lateral most aspect of the acetabular roof. The upper femoral epiphysis should be seen in the inferomedial quadrant, below Hilgenreiner's line, and medial to Perkin's line.
- If the nucleus of the femoral head is not visible because it is not ossified yet, the femoral metaphysis should be used.

Acetabular Coverage of the Femoral Head

The percent of the acetabular head coverage is calculated by dividing the distance between the acetabular floor line and a horizontal line extending from the iliac bone (d), by the distance between the acetabular floor and joint capsule line/femoral head diameter (D) multiplied by 100. A cutoff value of 50% is advocated (Fig. 3a) [9].

US Alpha-Beta Angle

- The American College of Radiology recommends that a standard US examination includes static images in two orthogonal planes and dynamic imaging.
- A coronal view in the "Graf standard plane" with three essential landmarks: the inferior border of the ilium, osseous acetabular roof, and labrum (Fig. 3a); transverse views of the flexed hip with and without stress and dynamic assessment to determine the position and stability of the femoral head, with a technique similar to the clinical Barlow examination.
- The Graf α and β angles are measured on a coronal image (Fig. 3a, b): the osseous acetabular roof angle (α angle) and acetabular cartilaginous (labrum) angle (β angle) [10, 11].

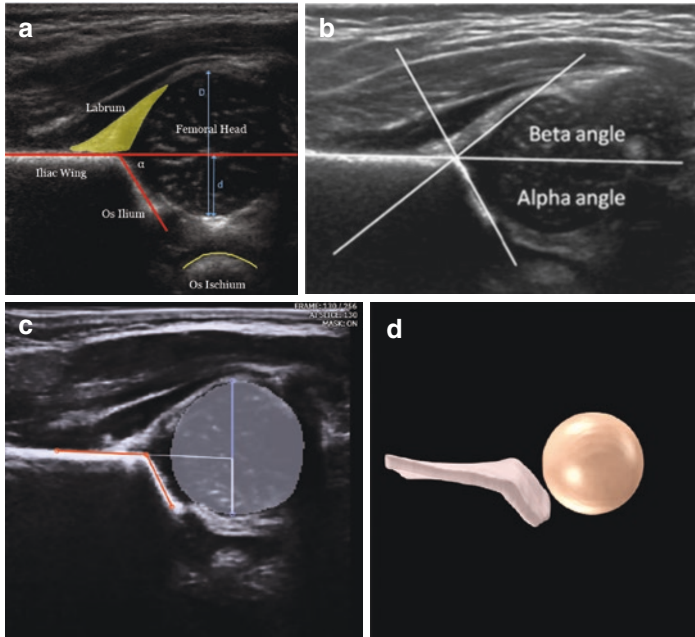


FIGURE 3 (a) Coronal ultrasound image in the “Graf standard plane” through the mid-hip joint with flat iliac wing, round femoral head, os ilium and os ischium visible, showing the measurement of the Graf α angle and acetabular coverage (d/D) and (b) Graf α (alpha) and β (beta) angles. (c) Automated identification of acetabulum and femoral head (segmentation) by artificial intelligence from 3D ultrasound, with (d) the corresponding 3D shape model. (Credit: Medo.ai)

- The modified Graf grading classification (four types listed in Table 2) is based on the α angle and degree of acetabular roof coverage [3].
- Three-dimensional (3D) US is an emerging imaging modality for infant’s hips. 3D shape indices can be generated to diagnose hip dysplasia more reliably and offer further insight into the 3D aspects of the deformity (Fig. 3c, d) [12].

TABLE 2 Modified Graf classification scale (Permission from Herregods et al. [1])

Graf		
type	Description	α and β angle
Type 1	Normal, mature hip with more than 50% acetabular roof coverage	α angle $\geq 60^\circ$ β angle $< 55^\circ$
Type 2a	Physiologic immaturity at younger than 3 months	α angle 50–59°
Type 2b	Immature at age 3 months or older	α angle 50–59°
Type 2c	Extremely deficient bony acetabulum; femoral head is concentric but not stable	α angle 43–49° β angle $< 77^\circ$
Type 2d	Femoral head is grossly subluxed and labrum is everted, increasing β angle	α angle difficult to measure but is approximately 43–49° β angle $> 77^\circ$
Type 3	Dislocated femoral head with shallow acetabulum	α angle $< 43^\circ$
Type 4	Dislocated femoral head with severely shallow, dysplastic acetabulum and inverted labrum	

- A scan protocol in which the whole hip joint is imaged by cine-sweep or 3D ultrasound improves reliability for non-expert users [13]. This type of scan is also amenable to automated analysis by artificial intelligence (AI). An AI app called Medo Hip using this approach has been cleared by US-FDA (<https://www.medo.ai/aria-hip>). In the future, population screening for hip dysplasia could be done by portable ultrasound performed by nurses and interpreted automatically by AI.

Medial Joint Space (Teardrop Distance)

- The medial joint space is used to determine lateral displacement of the femoral head on radiographs.
- It is defined as the distance measured from the medial edge of the femoral head ossification nucleus (where it is broadest just above the growth plate) to the adjacent acetabular wall.
- When the ossification nucleus is absent or asymmetric, measurement is made from the femoral neck metaphysis just below the growth plate.
- This measurement is best made on the frog-lateral projection [14].
- Normal range from 6 months to 11 years = 5–12 mm.
- In side-to-side comparison, the difference between measurements of the medial joint space should be less than 1.5 mm.

Shenton's Line

- Shenton's line is an imaginary curved line drawn along the inferior border of the superior pubic ramus (superior border of the obturator foramen) and along the inferomedial border of the neck of femur (Fig. 2).
- This line should be continuous and smooth.
- Interruption of the Shenton's line can indicate DDH or fractured neck of femur.

Perkin's Line

- Perkin's line is a line drawn perpendicular to Hilgenreiner's line, intersecting the most lateral aspect of the acetabular roof (Fig. 2).
- The upper femoral epiphysis should be seen in the inferomedial quadrant: it should lie below Hilgenreiner's line, and medial to Perkin's line.

- If the nucleus of the femoral head is not visible because it is not ossified yet, the femoral metaphysis should be used as reference.
- Lateral displacement of the femoral head occurs in DDH.

Lateral Center-Edge Angle (Wiberg)

- The lateral center-edge angle is a radiographic measurement to evaluate lateral coverage of the femoral head by the acetabulum.
- This angle is calculated on AP pelvic radiographs by drawing a best-fit circle for the inferior and medial margins of the femoral head. The angle is then measured between two lines drawn from the center of the circle, one running vertically along the longitudinal axis of the pelvis and the other one tangential to the lateral margin of the acetabular rim (Fig. 4).

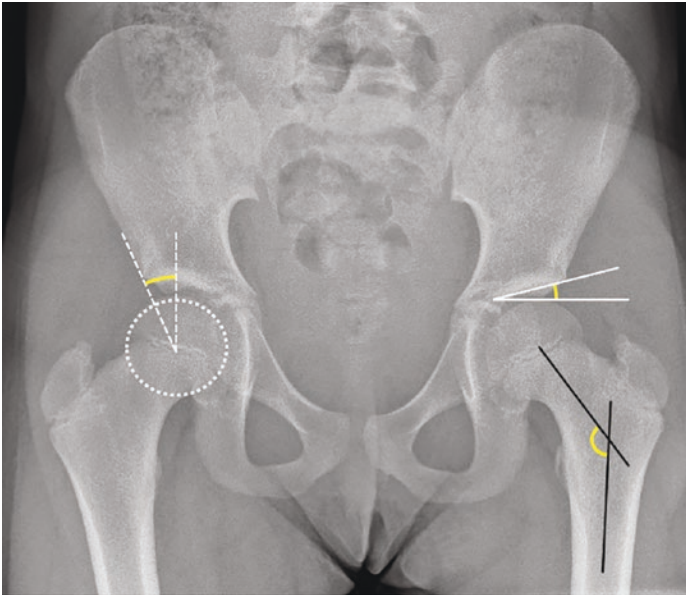


FIGURE 4 Anteroposterior radiograph showing the lateral center-edge angle (Wiberg) (dashed white lines), Tönnis angle (bold white lines), and femoral head-neck-shaft angle (bold black lines)

- Reference lateral center edge angles are 25° for children aged 0 (neonates) to 8 years and 32° for children older than 8 years to aged 18 years [15].
- Values $<20^\circ$ indicate acetabular dysplasia, between 20° and 25° : borderline acetabular dysplasia.
- Values of $>39^\circ$ indicate overcoverage (pincer-type impingement).

Vertical-Center-Anterior Angle

- The vertical-center-anterior angle is measured on a false profile view (Lequesne profile).
- This angle is used to evaluate anterior coverage of the femoral head and is formed by a vertical line through the femoral head center and a line connecting the femoral head center and anterior edge of the acetabular roof (Fig. 5).
- An angle of 20° – 25° indicates borderline dysplasia, and an angle of less than 20° indicates dysplasia [6].

Tönnis Angle

- The Tönnis angle is used to measure the acetabular surface and is formed by a horizontal line and a tangential line extending from the medial to lateral sclerotic edges of the acetabular roof (Fig. 4) [16].
- A Tönnis angle greater than 13° is abnormal.

Pubofemoral Distance

- Pubofemoral distance (PFD) is a reproducible measurement of hip instability; it is an easy sonographic screening test to avoid late diagnosis of developmental dysplasia of the hip.

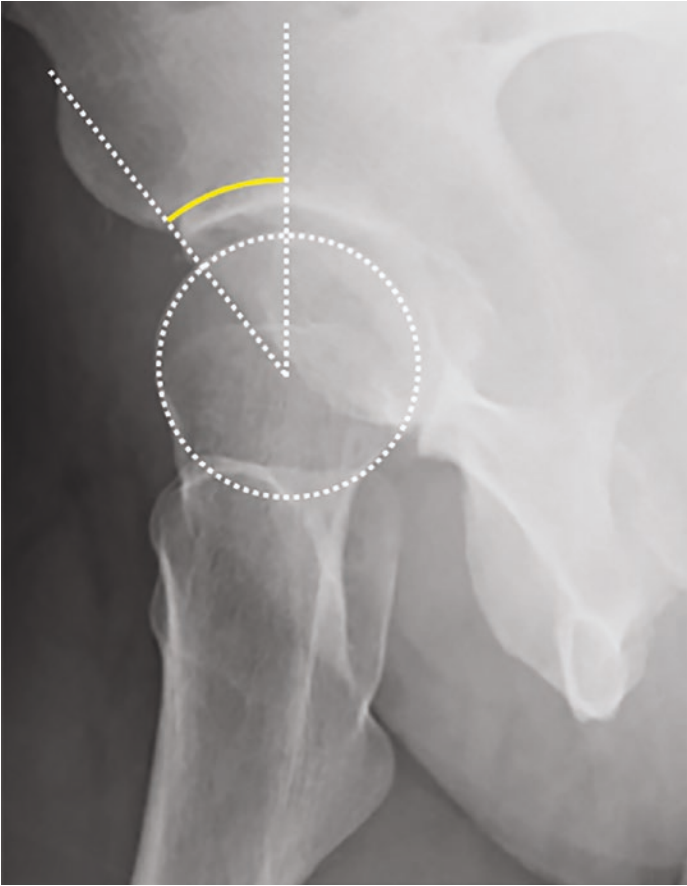


FIGURE 5 Image illustrating the vertical-center-anterior angle in the false profile view (Lequesne profile)

- PFD is measured between the medial margin of the epiphysis and the pubic bone (Fig. 6).
- PFD >6 mm (at the age of 1 month) or a difference >1.5 mm should lead to expert referral [17].

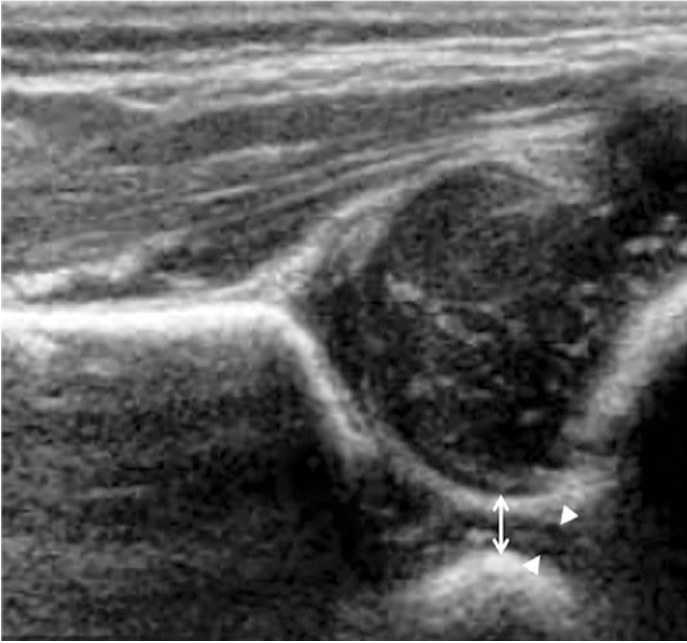


FIGURE 6 Ultrasound image illustrating the measurement of the pubofemoral distance (double-headed arrow) between the pubic bone and the femoral head. Arrowheads indicate the pubic cartilage thickness

Femoral Head-Neck-Shaft Angle

- The femoral head-neck-shaft angle is formed by the intersection of the femoral neck axis and femoral long axis (Fig. 4).
- The normal femoral neck-shaft angle ranges between 120° and 135° , and it decreases from 150° in infants to 120° in adults [18].
- In coxa vara, the angle is decreased to $<120^{\circ}$, and in coxa valga, the angle is increased to $>135^{\circ}$ (Fig. 7).
- External rotation of the femur should be avoided during patient positioning because as little as 7° of external rota-

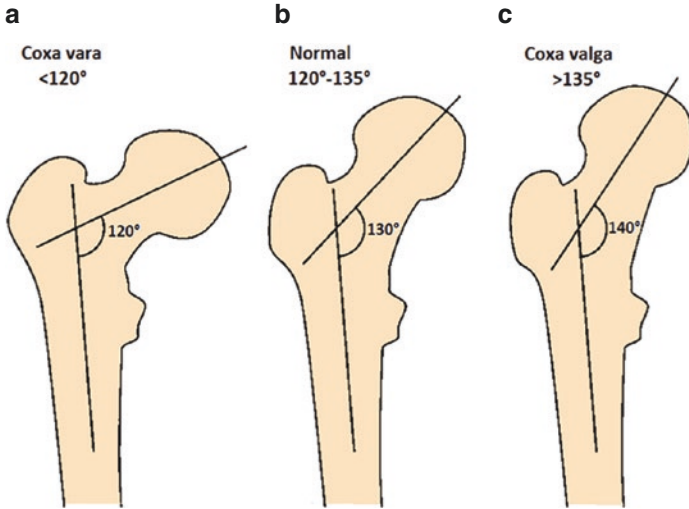


FIGURE 7 Femoral neck-shaft angle (black lines) in (a) coxa vara, (b) normal hip, and (c) coxa valga. (Permission from Herregods et al. [1])

tion may result in a $>10^\circ$ change in the measurement of the neck-shaft angle [19].

Slipped Capital Femoral Epiphysis (SCFE)

Klein's Line

- The Klein's line is a parallel line that is drawn along the lateral border of the femoral neck and intersects a small portion of the femoral epiphysis (FE) in normal hips.
- Hips with medial displacement of the FE lack this intersection (Fig. 8a). A 2-mm or greater difference in the epiphyseal width lateral to the Klein line between the hips strengthens the diagnosis of SCFE, with a sensitivity of 79% [20].

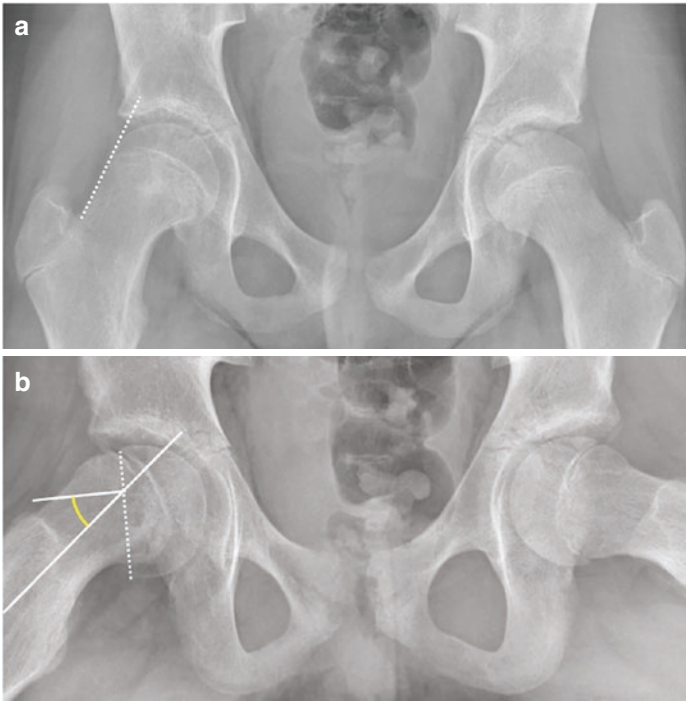


FIGURE 8 (a) Anteroposterior radiographs showing the Klein line and (b) Southwick SCFE measurement in the frog-leg lateral view

Southwick's Method

- The Southwick's method measures angular epiphyseal displacement by using the epiphyseal shaft angle on a frog-leg lateral radiograph.
- The epiphyseal shaft angle is formed between a line that is perpendicular to a line that connects the anterior and posterior margins of the FE and a line along the axis of the femoral shaft (Fig. 8b).

- Subtraction of the epiphyseal shaft angle value on the unaffected side from that on the affected side yields the epiphyseal slippage grade; in cases of bilateral slippage, a 12° angle is used as a normal reference.
- The severity of the slippage is classified as mild ($<30^\circ$ difference between angles), moderate (30° – 50° difference), or severe ($>50^\circ$ difference).
- Three-dimensional imaging should be considered for patients with limited hip flexion or external hip rotation [21].
- MRI may depict very early physeal changes without evidence of slippage during the “preslip” stage, when radiographs and CT scans show normal findings [22].

Femoroacetabular Impingement (FAI)

- There are two primary forms of FAI: cam type, which is a proximal femur abnormality, and pincer type, which is an acetabular component abnormality.
- For initial evaluation of the acetabulum, plain radiographs of the pelvis are recommended and an additional view of the femoral neck such as Dunn’s views, cross-table lateral, frog-leg lateral, or Meyer lateral for the assessment of the femoral head-neck junction [23].
- At anteroposterior radiography, characteristic cam impingement findings are sphericity and abnormal contour of the femoral head and femoral neck junction [6].
- Cross-table lateral or Dunn’s radiographic view of the hip or oblique axial (CT or MR) images along the femoral neck are used for evaluation of the extent of the cam deformity by measuring the anterior offset distance and the α angle.
- For pincer-type FAI, lateral center-edge angle, Tönnis angle, ilioischial line, crossover sign, posterior wall sign, and acetabular anteversion can be measured or observed.

Anterior Offset Distance

- The anterior offset is the distance from two parallel lines to the femoral neck axis measured on an axial view of the femur. One line is traced tangential to the anterior contour of the femoral head. The second line is traced to the point where the femoral head becomes aspherical (is no longer spherical), at the same point of the α angle (Fig. 9).
- An anterior offset distance shorter than 10 mm suggests FAI.

Alpha Angle

- The α angle is formed by the femoral neck axis and a line connecting the femoral head center to the point where the femoral head is no longer spherical (Fig. 9).
- An α angle of greater than 55° – 60° is abnormal.

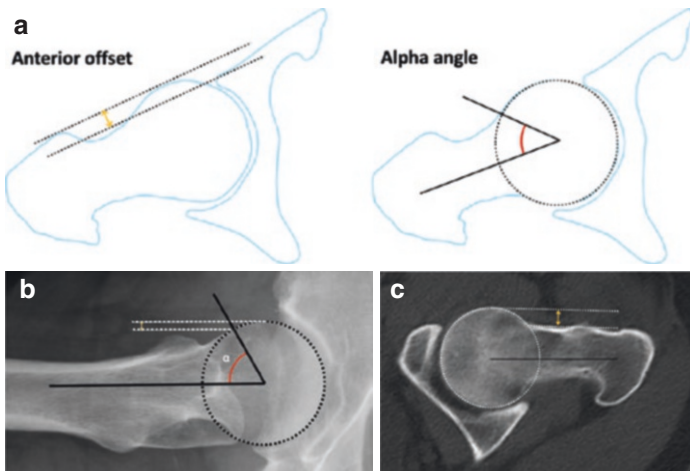


FIGURE 9 (a) Schematic drawings, (b) axial radiographic view, and (c) axial CT view of the proximal femur illustrating the anterior offset distance (orange double-headed arrows on a, b and c) and the alpha angle (black lines, angle depicted in red in a and b)

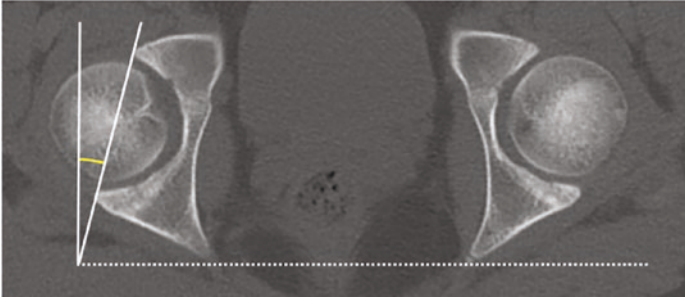


FIGURE 10 Measurements of acetabular anteversion

Acetabular Anteversion

- Axial CT image is used for measuring acetabular anteversion at the level of the femoral head center. Acetabular anteversion refers to the angulation of the line between the anterior and posterior acetabular margins and a line perpendicular to either the intercapital line or a horizontal line between the posterior pelvic margins at the sciatic notch level (Anda's method) (Fig. 10).

Lines: Arcuate/Acetabular Roof-Teardrop

- The arcuate line marks the border between the corpus and ala of the iliac bone. It runs inferior, anterior, and medial to the articular surface of the area corresponding to the acetabulum (Fig. 11).
- The iliopectineal, or arcuate line is a landmark for the anterior column. The ilioischial line is a landmark for the posterior column. The acetabular roofline and “teardrop” are a landmark for the medial portion of the acetabulum.
- The acetabular teardrop (U-figure, “Köhler's teardrop”) represents the projection of a bony ridge along the floor of the acetabular fossa (Fig. 11).
- An increased space of >11 mm increased distance between the pelvic teardrop and the femoral head or >2 mm in comparison to the contralateral hip indicates hip joint effusion [24].



FIGURE 11 Anteroposterior radiograph showing the ilioischial line (dashed white line), the acetabular roof line (dashed black line), and acetabular “teardrop.” The bold white line is the posterior rim of the acetabulum, and the bold black line is the anterior acetabular rim

Pelvic Tilt

- The pelvic tilt is easiest measured on a lateral view of the pelvis. Pelvic tilt is measured from the angle between a vertical line and the line joining the mid point of the upper sacral endplate and the hip axis (Fig. 12).
- Normal values for boys are $6.5 \pm 7.5^\circ$ (range: -10.2 to 30.0). Normal values for girls are $8.5 \pm 8.3^\circ$ (range: -17.2 to 29.7). Pelvic tilt tends to increase during growth.
- Numerous methods have been described for the estimation of pelvic tilt on AP pelvis radiograph. The most reliable estimator that has been described is the sacrococcygeal

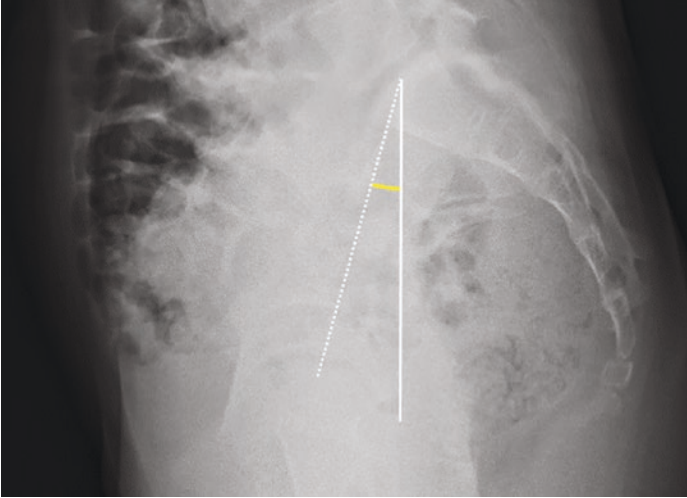


FIGURE 12 Lateral pelvic radiograph illustrating measurement of pelvic tilt. This is the angle between the vertical (bold white line) and a line joining the mid point of the upper sacral endplate and the hip axis (dotted white line)

joint to symphysis pubis distance; this is the distance between the midportion of the sacrococcygeal joint and the upper border of the public symphysis. The normal value is about 32 mm in men and 47 mm in women.

- Variation in the pelvic tilt on radiographs influences the acetabular measurements such as the acetabular index, lateral center-edge angle, crossover sign, Tönnis angle, or acetabular coverage [25–28].

Pubic Symphyseal Width

- The transverse width of the symphysis pubis using a focus-film distance of 1 m is measured to the nearest tenth of a millimetre.
- Normal values gradually decrease from 7.4 ± 1.3 mm aged 0–6 months to 5.4 mm aged 16 years [9].

References

1. Herregods N, Vanhoenacker FM, Jaremko JL, Jans L. Update on pediatric hip imaging. *Semin Musculoskeletal Radiol.* 2017;21:561–81. <https://doi.org/10.1055/s-0037-1606134>.
2. Lee MC, Ebersson CP. Growth and development of the child's hip. *Orthop Clin North Am.* 2006;37(02):119–32. <https://doi.org/10.1016/j.ocl.2005.12.001>.
3. Starr V, Ha BY. Imaging update on developmental dysplasia of the hip with the role of MRI. *AJR Am J Roentgenol.* 2014;203(06):1324–35.
4. Bracken J, Tran T, Ditchfield M. Developmental dysplasia of the hip: controversies and current concepts. *J Paediatr Child Health.* 2012;48(11):963–72; quiz 972–973.
5. Bracken J, Ditchfield M. Ultrasonography in developmental dysplasia of the hip: what have we learned? *Pediatr Radiol.* 2012;42(12):1418–31.
6. Silva MS, Fernandes ARC, Cardoso FN, Longo CH, Aihara AY. Radiography, CT, and MRI of hip and lower limb disorders in children and adolescents. *Radiographics.* 2019;39:779–94. <https://doi.org/10.1148/rg.2019180101>.
7. Grissom LE. The pelvis and hip: congenital and developmental conditions. In: Stein-Wexler R, Wootton-Gorges S, Ozonoff M, editors. *Pediatric orthopedic imaging.* Berlin: Springer; 2015. p. 273–318.
8. Caffey in Ozonoff MB. *Pediatric orthopedic radiology.* Philadelphia: W.B. Saunders; 1992. p. 181.
9. Keats T, Siström S. *Atlas of radiologic measurement.* 7th ed. Philadelphia, PA: Mosby; 2001.
10. American Institute of Ultrasound in Medicine. AIUM practice guideline for the performance of an ultrasound examination for detection and assessment of developmental dysplasia of the hip. *J Ultrasound Med.* 2013;32(07):1307–17.
11. Graf R. Classification of hip joint dysplasia by means of sonography. *Arch Orthop Trauma Surg.* 1984;102(04):248–55.
12. Jaremko JL, Mabee M, Swami VG, Jamieson L, Chow K, Thompson RB. Potential for change in US diagnosis of hip dysplasia solely caused by changes in probe orientation: patterns of alpha-angle variation revealed by using three-dimensional US. *Radiology.* 2014;273(03):870–8.

13. Mostofi E, Chahal B, Zonoobi D, et al. Reliability of 2D and 3D ultrasound for infant hip dysplasia in the hands of novice users. *Eur Radiol.* 2019;29(3):1489–95. <https://doi.org/10.1007/s00330-018-5699-1>.
14. Eyring et al. in reference: Ozonoff MB. *Pediatric orthopedic radiology.* W.B. Saunders Company: Philadelphia. 1992. p. 181. (Used with permission from M.B. Ozonoff; publisher's permission requested); 1965.
15. Waldt S. Hip. In: Waldt S, Woertler K, editors. *Measurements and classifications in musculoskeletal radiology.* Munich: Thieme; 2013. p. 10–47.
16. Beltran LS, Rosenberg ZS, Mayo JD, et al. Imaging evaluation of developmental hip dysplasia in the young adult. *AJR Am J Roentgenol.* 2013;200(5):1077–88.
17. Tréguier C, Chapis M, Branger B, et al. Pubo-femoral distance: an easy sonographic screening test to avoid late diagnosis of developmental dysplasia of the hip. *Eur Radiol.* 2013;23(3):836–44. Epub 2012 Oct 20. <https://doi.org/10.1007/s00330-012-2635-7>.
18. Hubbard AM. Imaging of pediatric hip disorders. *Radiol Clin North Am.* 2001;39(04):721–32.
19. Kay RM, Jaki KA, Skaggs DL. The effect of femoral rotation on the projected femoral neck-shaft angle. *J Pediatr Orthop.* 2000;20(6):736–9. <https://doi.org/10.1097/00004694-200011000-00007>.
20. Green DW, Moge kwu N, Scher DM, Handler S, Chalmers P, Widmann RF. A modification of Klein's line to improve sensitivity of the anterior-posterior radiograph in slipped capital femoral epiphysis. *J Pediatr Orthop.* 2009;29(5):449–53.
21. Jones CE, Cooper AP, Doucette J, et al. Southwick angle measurements and SCFE slip severity classifications are affected by frog-lateral positioning. *Skeletal Radiol.* 2018;47(1):79–84.
22. Fayad LM, Johnson P, Fishman EK. Multidetector CT of musculoskeletal disease in the pediatric patient: principles, techniques, and clinical applications. *Radiographics.* 2005;25(3):603–18.
23. Albers CE, Wambeek N, Hanke MS, Schmaranzer F, Prosser GH, Yates PJ. Imaging of femoroacetabular impingement-current concepts. *J Hip Preserv Surg.* 2016;3(4):245–61. <https://doi.org/10.1093/jhps/hnw035>.
24. Yochum and Rowe. *Essentials of skeletal radiology.* LWW. ISBN: 0781739462.

25. Mac-Thiong JM, Labelle H, Berthonnaud E, et al. Sagittal spinopelvic balance in normal children and adolescents. *Eur Spine J*. 2007;16(2):227–34. <https://doi.org/10.1007/s00586-005-0013-8>.
26. Tannast M, Siebenrock KA, Anderson SE. Femoroacetabular impingement: radiographic diagnosis—what the radiologist should know. *Am J Roentgenol*. 2012;188(6):1540–52.
27. Henebry A, Gaskill T. The effect of pelvic tilt on radiographic markers of acetabular coverage. *Am J Sports Med*. 2013;41(11):2599–603.
28. Hamano D, Yoshida K, Higuchi C, et al. Evaluation of errors in measurements of infantile hip radiograph using digitally reconstructed radiograph from three-dimensional MRI. *J Orthop*. 2019;16(3):302–6. <https://doi.org/10.1016/j.jor.2019.05.004>.